Hydrophobic channels produced by micelle-structured CTAB inside MCM-41 mesopores: A unique trap for the hazardous hormone ethinyl estradiol

Tatiana A. Ribeiro-Santos [a], Fernando Fulgêncio Henriques [a], Jhonny Villarroel-Rocha [b], Mateus Carvalho Monteiro de Castro [a], Welington Ferreira Magalhães [a], Dario Windmöller [a], Karim Sapag [b], Rochel Montero Lago [a], Maria Helena Araujo [a,*]

[a] Departamento de Química, Instituto de Ciências Exatas, Universidade Federal de Minas Gerais, Belo Horizonte, MG 31270-901, Brazil
[b] Instituto de Física Aplicada, CONICET, Universidad Nacional de San Luis, San Luis, Argentina

HIGHLIGHTS

- Mesoporous MCM-41 with hydrophobic mesoporous cavities.
- Hydrophobic cavities for the efficient removal of the hormone ethinyl estradiol.
- Hydrophobic cavities formed by the cetyl trimethylammonium bromide (CTAB).

GRAPHICAL ABSTRACT
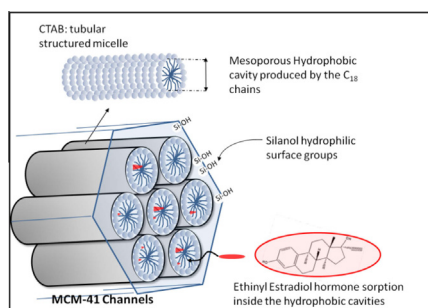
ABSTRACT

In this work, mesoporous hydrophobic cavities produced by a micelle structured CTAB (cetyl trimethylammonium bromide) trapped inside MCM-41 pores were used for the efficient removal of the hazardous hormone contaminant ethinyl estradiol (EE) present in water. The MCM-41 structure was prepared using different CTAB/Si molar ratios, i.e. 0.07, 0.12, 0.17, and 0.27. TG, SEM, TEM, BET, IR, elemental analysis, contact angle and positron annihilation spectroscopy showed that the MCM-41 silica structure is completely filled with trapped CTAB molecules (47–58 wt%) which results in no porosity and very low surface areas of $1-5 \ m^2 \ g^{-1}$. These materials showed high efficiency to remove EE from aqueous solution whereas pure MCM-41 (without CTAB) with high porosity and a surface area of $1333 \ m^2 \ g^{-1}$ showed no adsorption. These results are discussed in terms of EE sorption into the hydrophobic environment created by the CTAB trapped molecules inside the mesoporous cavities of MCM-41.

© 2015 Elsevier B.V. All rights reserved.

1. Introduction

Emergent contaminants, especially endocrinous disruptors, even at extremely low concentrations, have severe adverse effects in different organisms such as reduced sperm count, increased incidence of breast, testicular and prostate cancer and endometriosis [1–7]. Ethinyl estradiol (EE) is considered one of the most

* Corresponding author at: Departamento de Química – Universidade Federal de Minas Gerais – UFMG, Av. Antônio Carlos, 6627, Pampulha, Belo Horizonte, MG CEP 31270-901, Brazil. Tel.: +55 31 3409 7557.
E-mail address: maria.araujo@pq.cnpq.br (M.H. Araujo).

hazardous endocrinous disruptor [8–11] widely used as contraceptive in hormonal treatments in humans and animals. EE is commonly eliminated in domestic sewages, industrial wastewaters [6,9] and common biological treatments are not efficient to remove the hormone [10–12]. Different methodologies such as advanced oxidation processes (Fenton, O_3, UV) [13–15] and reversed osmosis [16] have been investigated for the elimination of EE [17]. Adsorption on activated carbon (AC) has been reported as a promising way to remove hormones and other endocrinous disruptors from water [3,8,18]. However, diffusion limitations seem to hinder the adsorption of EE on typical microporous activated carbons due to the relatively large EE molecule (estimated diameter *ca.* 12 Å) [1].

It has also been suggested that a hydrophobic/hydrophilic balance is very important for the efficient adsorption of the EE molecules. The hydrophobic character favors the adsorption of the EE hormone, whereas hydrophilic features are important to promote a good interaction and interface of the adsorbent with the aqueous medium.

In this work, the mesoporous MCM-41 was used to create hydrophobic mesoporous cavities for the efficient removal of the hormone EE. These hydrophobic cavities are formed during the MCM-41 synthesis due to the presence of the template cetyl trimethylammonium bromide (CTAB) which is located and trapped inside the mesoporous structure (Fig. 1) [19]. The CTAB tubular structured micelle formed inside the MCM-41 has C_{16} hydrocarbon chains forming strongly hydrophobic channels large enough to interact with EE molecules and remove them by a sorption mechanism [20]. On the other hand, the external surface of the preformed MCM-41 silica structure has silanol groups producing a more hydrophilic surface which provides a good interaction with the aqueous medium.

2. Materials and methods

2.1. Synthesis of sorbents

The synthesis of the MCM-41 was carried out using a suspension of CTAB (Sigma Aldrich) in deionized water (108 mL) mixed with NaOH (Vetec) (54 mL, 1.35 mmol) under vigorous magnetic stirring until a clear solution was obtained. Subsequently, 20 mL

(0.09 mol) of tetraethyl orthosilicate, TEOS (Merck), was added dropwise to form an emulsion which was magnetic stirred for 24 h. The obtained solids were separated by vacuum filtration, washed with deionized water until the conductivity was below $10 \mu S cm^{-1}$ and oven-dried for 12 h at 60 °C, yielding the pure sorbents. To obtain the other sorbents (M47–M58), the following molar ratios were used: M47 (0.07 CTAB: 1 TEOS: 0.6 NaOH: 100 H_2O), M50 (0.12 CTAB: 1 TEOS: 0.6 NaOH: 100 H_2O), M52 (0.17 CTAB: 1 TEOS: 0.6 NaOH: 100 H_2O) and M58 (0.27 CTAB: 1 TEOS: 0.6 NaOH: 100 H_2O).

The best sorbent (M52) was submitted to calcination at 550 °C for 6 h with heating rate of 1 °C min^{-1} to generate the $M_{550°C}$ material.

2.2. Characterization of materials

The samples, as KBr pellets, were characterized by Fourier transform infrared spectroscopy (FTIR) (PerkinElmer GX FTIR) in the spectral range of 400–4000 cm^{-1} (Fig. S1). The TG/DTG (TG DTG Shimatzu-60H were performed in air, with a heating rate of 10 °C min^{-1} to 900 °C). Measurements of nitrogen (99.999%) sorption/desorption at 77 K were carried out using volumetric sorption equipment (Autosorb-1MP, Quantachrome Instruments). Prior to such measurements, the samples were degassed at 150 °C for 12 h until the residual pressure was less than 0.5 Pa. The Brunauer, Emmett and Teller (BET) method [21] was used to estimate the specific surface area (S_{BET}) of the samples, using the nitrogen adsorption data over the relative pressure range 0.05–0.12 P/P_0 for MCM-41. XRD measurements were performed on a Rigaku D-MAX IIIC diffractometer using Ni-filtered Cu Kα radiation over the 2θ range 1–10°. SEM images were obtained on a Quanta 200 FEG – FEI electron microscope and TEM images were obtained on G2–20 – SuperTwin Tecnai FEI electron microscope. The contact angle was obtained using 50 mg tablets. A 15 μL water drop was placed on the pads and, using a digital camera, an image was taken. From the picture it was possible to calculate the contact angle between the water droplet and sorbent sample.

PALS measurements were performed at 295 using a fast–fast coincidence system (ORTEC), with a time resolution of 230 ps given by ^{60}Co prompt curve. The ^{22}Na (Perkin Elmer) positron source, with approximately 20 μCi activity, was sandwiched between
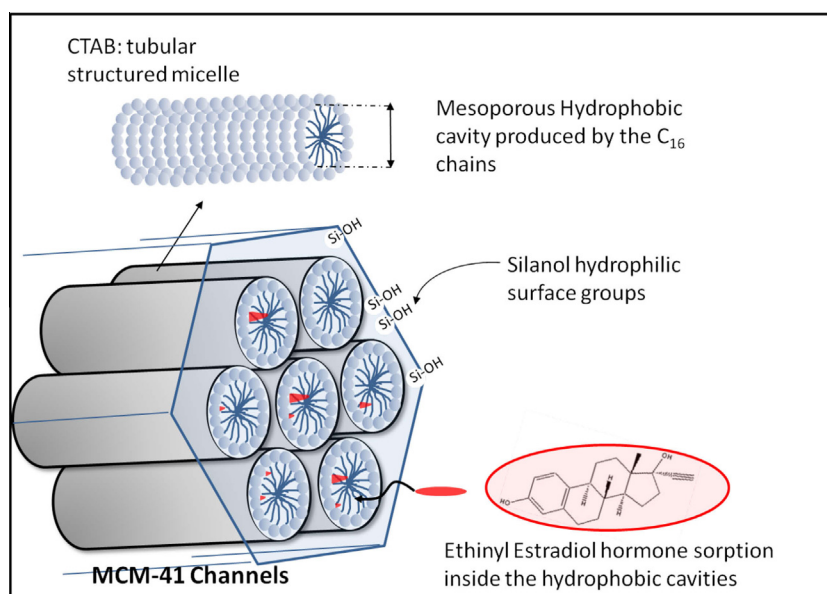

Fig. 1. Simplified schematic representation of the hydrophobic mesoporous cavities formed in the MCM-41 structure and the adsorption of EE.

two 7.6 μm thick kapton foils, and the source correction was approximately 20%. The lifetime spectra, with minimum of six measurements for each sample, were resolved with three or four components using the Positronfit-Extended program [22]. Lifetimes, τ_i, and associate relative intensities, I_i (%), were obtained, where i = 1, 2, 3 and 4 refers, respectively, to p-Ps, free positron, o-Ps in the bulk and o-Ps trapped in larger vacancies, such as mesopores. Since the average lifetime of p-Ps is lower than the equipment's resolution, the τ_1 parameter is fixed at 0.120 ns. Such artifice does not alter the value of the other parameters and reduces the correlation between the fitted parameters.

2.3. Application

2.3.1. Sorption test of ethinyl estradiol

Sorption isotherms were obtained using 10 mg of the sorbent (M47–M58) and 10 mL of different concentrations solutions (0, 5, 10, 15, 20 and 25 mg L^{-1}) for ethinyl estradiol (EE). The mixtures were kept under stirring of 180 rpm for 24 h at room temperature. The determination of the equilibrium concentration was carried out in an UV–visible equipment (Biosystems, Model SP 2550 UV) (λ = 280 nm). For comparison, the calcinated M$_{550°C}$ sorption isotherm was also obtained.

2.3.2. Sorption kinetic

Sorption kinetic was obtained using 10 mg of sorbent (M52) and 10 mL of a 20 ppm EE solution. The system was kept under stirring (180 rpm) and the concentration was measured along the time, using a UV–visible equipment, until saturation of the sample.

2.3.3. Total organic carbon

To evaluate the leach of the CTAB a M52 sample, in water, was left stirring for 1 h and, after filtration, the total organic carbon (TOC) was determined using a Shimadzu TOC-V CPH.

2.3.4. Effect of pH

The effect of pH in the sorption capacity was evaluated adjusting the pH of the solution to 2, 6, 10 and 14. The test was carried out using 10 mg of M52 and 10 mL of a 20 ppm EE solution. The solutions with the sorbents were kept under stirring for 60 min and then the concentrations were measured using a UV–visible equipment.

2.3.5. Isosteric heat

The isosteric heat of sorption (Q_{st}) was obtained applying the Clausius–Clapeyron Eq. (1) to the isotherms data at different temperatures, 10, 28 and 40 °C [23].

$$Q_{st} = RT^2 \left(\frac{d(\ln P)}{dT} \right)_\theta \qquad (1)$$

2.3.6. Reuse

It is interesting to have a sorbent that efficiently removes contaminants and can be reused. Thus, the M52 ability to be reused was tested. For this, 200 mg of the sorbent (M52) were placed in contact with 200 mL of EE 20 ppm for 24 h under 180 rpm stirring. The supernatant was analyzed by UV–visible (280 nm). The remaining solution was removed from EE, and the sorbent was washed with acetonitrile and centrifuged. The supernatant was removed and dried. Subsequently, 200 mL of EE 20 ppm were added and the procedure repeated until saturation of the material.

3. Results and discussion

The CTAB content determined by TG/DTG analyses and BET surface area are shown in Supplementary material (Fig. 2 and Table S1). TG profiles showed weight losses ranging from 47 up to 58% at temperatures of 140–350 °C due to the loss of CTAB. These samples have been named according to their CTAB content, *i.e.* M47, M50, M52 and M58. TG also suggests that the MCM-41 thermally treated at 550 °C/6 h completely lost the CTAB resulting in a mesoporous material with high surface area of 1333 m^2 g^{-1}. On the other hand, all other non-heated materials showed very low surface area (1–5 m^2 g^{-1}) due to the presence of the CTAB inside the porous structure of the silica. The formation of the MCM-41 mesoporous structure in these materials (without any thermal treatment) was confirmed by low angle X-ray diffraction patterns (Fig. 2a), with the presence of typical hexagonal cell peaks. This result may be compared with the low angle X-ray diffraction pattern for the MCM-41 thermally treated sample, M$_{550°C}$ (Fig. 2b) [24].

The removal of CTAB from all these materials produced by simple thermal treatment at 550 °C led to the typical mesoporous MCM-41 with surface areas between 800–1500 m^2 g^{-1} and pore diameter distribution centered in the range 30–40 Å (Fig. S3).

SEM images of the composite M47 showed the presence of agglomerates of amorphous particles. The other composites M50, M52 and M58 revealed agglomerates composed of fairly well defined particles with dimensions around 10–30 μm. It is interesting to observe that all the obtained TEM images presented typical fringes related to the MCM-41 structure, Fig. 3.

Positron annihilation lifetime spectroscopy (PALS) was used to investigate the free volumes size of the silica cavities filled with CTAB. The samples formed significant amounts of Ps (I_3 > 20%)
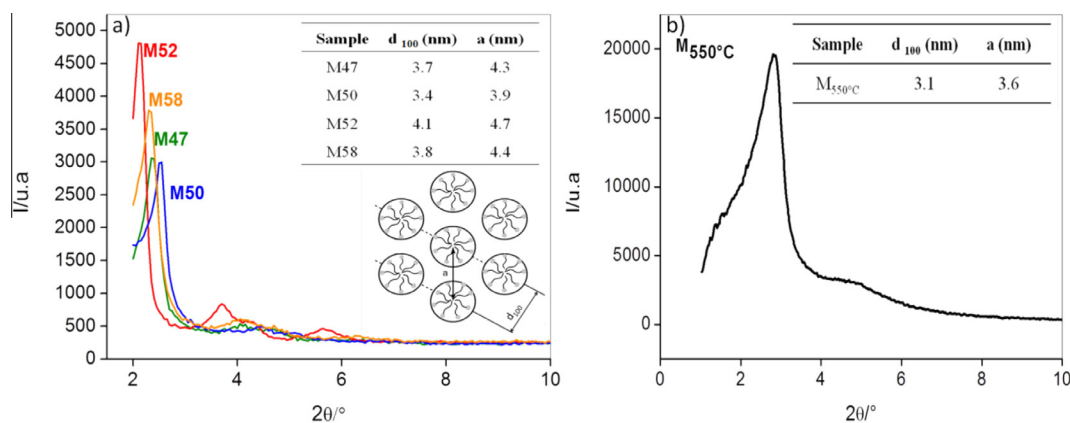

Fig. 2. Low angle XRD diffraction patterns for (a) the obtained composites and (b) the calcinated MCM-41 sample M$_{550°C}$.

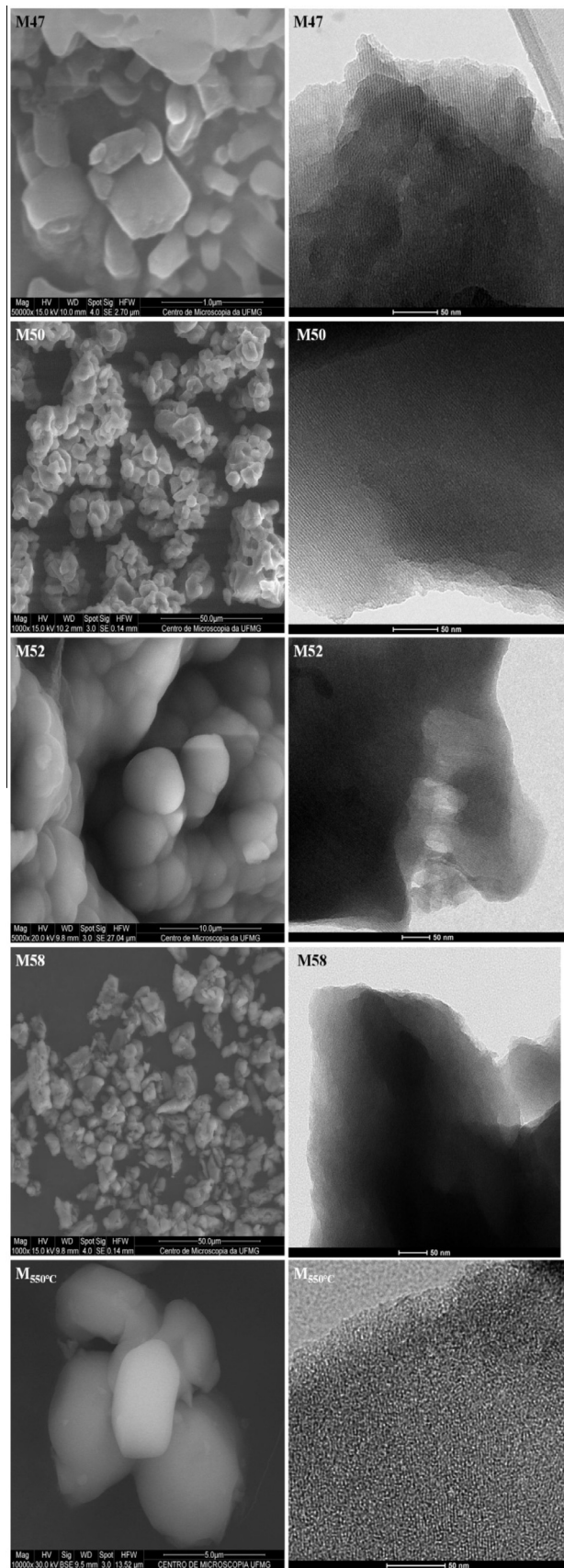**Fig. 3.** SEM and TEM images obtained for the samples M47, M50, M52, M58 and $M_{550°C}$.

and the obtained τ_3 values were used to estimate the size of the free volumes present in the samples (see Supplementary Material – 1.4). PALS results suggested that the MCM-41 sample without CTAB (sample treated at 550 °C for 24 h, $M_{550°C}$) presents large average free volumes ($V = 2644$ Å^3), which is related to the empty mesoporous cavities (30–40 Å). On the other hand, all the CTAB/MCM-41 composites clearly indicated much smaller free volume spaces varying from 183 to 192 Å^3, which probably correspond to the molecular interstices within CTAB molecules. These results suggest that the MCM-41 cavities are filled with CTAB molecules, leaving only 7%, approximately, of the MCM-41 mesoporous volumes available for the sorption of the EE molecules.

The sorption capacity of all prepared materials were investigated using the hormone ethinyl estradiol (EE) to select the best sorbent for further studies. The sorption isotherms of ethinyl estradiol (EE) in the different CTAB/MCM-41 materials are shown in Fig. 4.

The composites M47, M50 and M58 showed high removal of EE *ca.* 6–7 mg g^{-1}, while the thermally treated MCM-41 ($M_{550°C}$), with very high surface area (1333 m^2 g^{-1}), does not remove any EE from the aqueous solution.

The best sorption results were obtained for the M52 material, 9.5 ($\pm$0.4) mg g^{-1}, which is higher than the results obtained with other materials of similar surface area, such as, inactivated sewages (2.6 mg g^{-1}) [25], activated carbon obtained from used coffee powder (0.007 mg g^{-1}) [26] and sorption column (7.8 mg g^{-1}) [27]. Compared with different carbon forms, *e.g.* nanotubes and activated carbon, the sorption capacity is lower, *e.g.* 115 mg g^{-1} [28] and 200 mg g^{-1} [29]. However, if a comparison with a data normalized by surface area is carried out, the sorption capacity of the M52 is much higher, for example: M52 (1.9 mg m^{-2}), carbon nanotubes (0.10 mg m^{-2}) [30], activated carbon (0.046 mg m^{-2}) [30] and carbon/chrysotile composite (0.53 mg m^{-2}) [30].

Considering that the best results were obtained with the M52 material, different experiments were carried out to further understand the sorption process on this material. The kinetic curves of sorption for EE (Fig. S4 Supplementary material) showed that after 60 min the M52 is saturated. The effect of pH on the EE sorption on M52 was also investigated. It was observed a lower sorption capacity of 7 mg g^{-1} at pH 2, which increased to 10–12 mg g^{-1} in the pH range 6–10. On the other hand, at pH 14, the sorption significantly decreased to 5 mg g^{-1} (Fig. S5 Supplementary material).
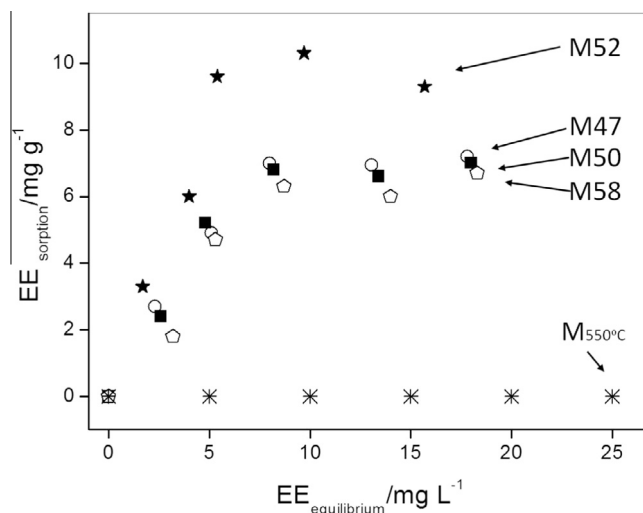

Fig. 4. Sorption isotherms of EE on CTAB/MCM-41 composites.

The sorption isotherms, of EE for the M52 material, were carried out at different temperatures (Fig. 5), 10, 28 and 40 °C. It is possible to observe a strong dependence of the sorption capacity with the temperature, where the sorption capacity decreases with the increase of the temperature.

Fig. 6 shows the dependence of the isosteric heat sorption (Q_{st}) with the amount of EE sorbed. The estimated Q_{st} value of 6.6 kJ mol^{-1} is in the range expected for physisorption processes, e.g. lower than 40 kJ mol^{-1}. For ordinary physisorption processes it is expected a decrease of the Q_{st} when the sorption increases [31,32]. However, for the sorption of EE on the M52 it is observed an increase of Q_{st} with the increase of EE sorbed which suggests that the sorption of the second molecule of EE is more favorable than the first. The non-linearity of the Van't Hoff plot (Fig. S6 Supplementary material) indicates that the heat of sorption is not constant and it increases with the increase of the temperature.

Considering the sorption capacity of the M52 material (12 mg g^{-1}), its low specific area, 5 m^2 g^{-1}, and the behavior of the isosteric heat, it is possible to suggest that EE is sorbed mainly inside the MCM-41 tubes filled with very orderly micellar CTAB molecules.
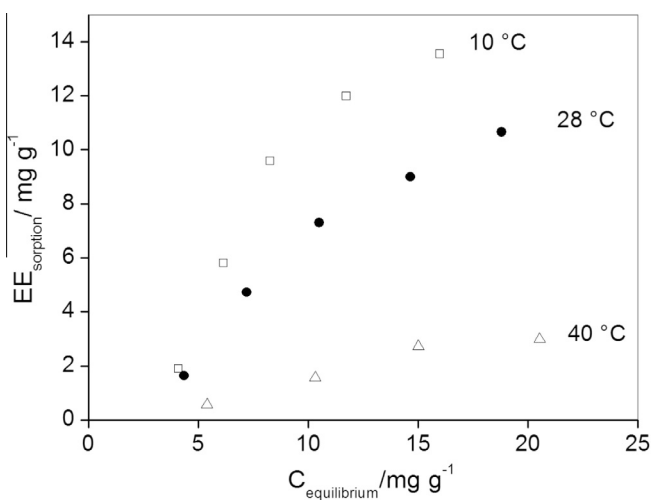
The CTAB/MCM-41 composite M52 was tested for consecutive reuse sorption experiments. After sorption the CTAB/MCM-41 was washed with acetonitrile to remove the EE sorbed and used again for new sorption experiments, these results are shown in Fig. 7.

It is possible to observe that on the second and third use of the M52 the removal capacity decreased from 74% to ca. 62% whereas the fourth use, a more significant decrease was observed, i.e. 40%. This lower EE removal capacity is related to the decrease of CTAB content from 52% to 32% (see TG of the reused M52 in Fig. S8) during the extraction with acetonitrile.

The effect of CTAB trapped inside the MCM-41 cavity on the EE sorption was investigated by controlled removal of the tensioactive molecule by thermal treatment. Upon treatment at 250, 300, 350 and 550 °C under air atmosphere the CTAB content of the MCM-41 silica decreased to 52%, 27%, 15%, 11% and 0%, respectively. Fig. 8 clearly shows that the EE sorption capacity is strongly dependent on the CTAB content inside the MCM-41 structure.

In order to further investigate the interaction of the hormone (EE) with CTAB, different materials were prepared, i.e. CTAB impregnated on the surface of MCM-41 (MCM + CTAB) and CTAB impregnated on the surface of a microporous silica (SiO$_2$ + CTAB), (SiO$_2$, surface area of 500 m^2 g^{-1}). The obtained results showed a strong decrease on the EE removal for the MCM + CTAB (21% of

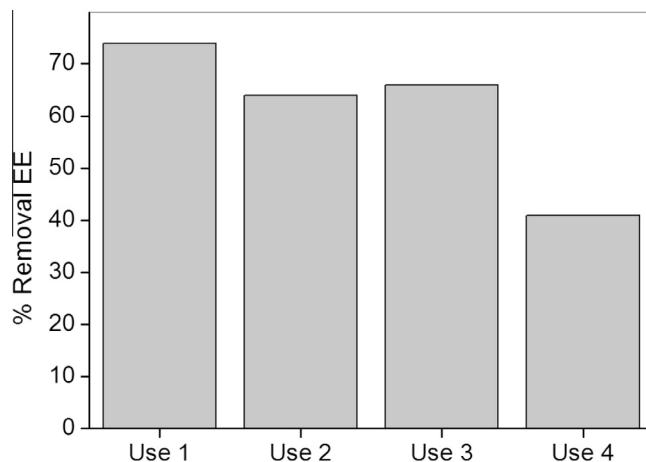Fig. 5. Sorption isotherms of EE on M52 at different temperatures.

Fig. 7. Reuse of the sorbent M52 for sorption of EE.

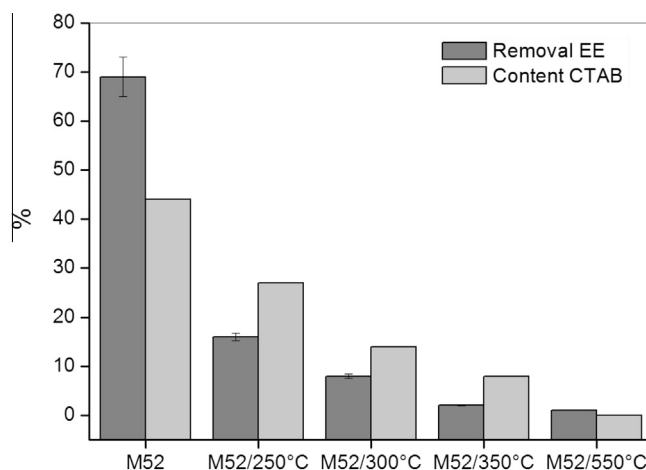Fig. 6. The isosteric heat of sorption on M52 material.

Fig. 8. Comparison between the % of EE removal (solution of 20 ppm EE) with the % of CTAB present in the materials.
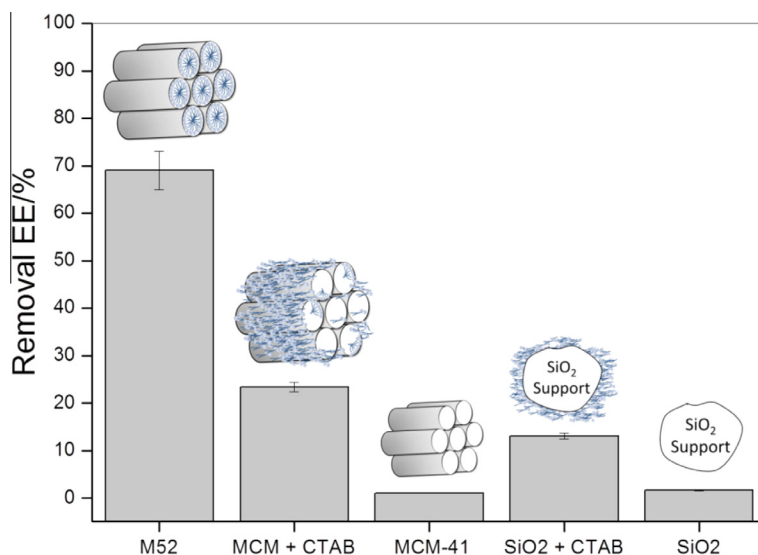
Fig. 9. Percentage of EE sorption in different forms of CTAB, *i.e.* entrapped inside the MCM-41 (M52), impregnated on the surface of MCM-41 (MCM + CTAB) and on microporous SiO_2 (SiO_2 + CTAB).

CTAB, Fig. S7a) and SiO_2 + CTAB (22% of CTAB, Fig. S7b) materials compared with the composite M52 (Fig. 9).

These results clear indicated that the CTAB molecules entrapped inside the mesoporous cavity of MCM-41 is important for the sorption of EE. Apparently, these CTAB molecules are organized as a tubular structured micelle well packed inside the cavities which results in materials with very low surface area and near no porosity. In fact, preliminary studies with the composite M52 showed that only 2% of the CTAB can be leached in water. The packing of the CTAB molecules likely forms strongly hydrophobic environments produced by the long $C_{16}H_{37}$ chains inside mesoporous cavity. The EE molecule is fairly hydrophobic (water solubility of $20\ mg\ L^{-1}$, 20 °C) and should interact very well with these hydrophobic environment. Therefore, it is proposed that the EE molecule diffuses into the M52 cavity and is absorbed/adsorbed in the hydrophobic environment created by the packing of the $C_{16}H_{37}$ chains inside the mesoporous cavity. It seems that the impregnated non-organized CTAB (MCM + CTAB or SiO_2 + CTAB) inside and outside the pore structure does not provide this hydrophobic environment for the EE sorption.

Another interesting feature of the M52 composite is the amphiphilic behavior. The pure MCM-41 treated at 550 °C ($M_{550°C}$) showed a low contact angle of *ca.* 25° suggesting very good interaction with water. This interaction is due to the silica and Si–OH surface groups. On the other hand, the composites M47, M50 and M52 showed higher contact angles of *ca.* 60°, 70° and 76°, respectively, suggesting a more hydrophobic character whereas the M58 sample a slightly more hydrophilic character with a contact angle of 45°. It is interesting to note that the EE sorption process is significantly related with the obtained contact angles (Fig. 10).

4. Conclusion

MCM-41 prepared by hydrothermal synthesis naturally produces mesoporous cavities containing trapped the CTAB template. The CTAB molecules completely fill the mesoporous cavities creating a unique hydrophobic environment formed by the tubular structured micelle whereas the silica surface is more hydrophilic due to the presence of silanol groups. This combination produces a good adsorbent/absorbent material for the hazardous hormone contaminant ethinyl estradiol (EE). It is suggested that the large EE molecule can enter the mesoporous cavity and accommodate in the very hydrophobic environment created by the organized $C_{16}H_{37}$ chains. The materials can be partially regenerated by simple selective extraction of EE by acetonitrile.

Acknowledgements

Appendix A. Supplementary data

Supplementary data associated with this article can be found, in the online version, at http://dx.doi.org/10.1016/j.cej.2015.08.029.

Fig. 10. Comparison between the contact angle and the removal percentage of EE.

References

[1] A.D. Purceno, A.P.C. Teixeira, N.J.D. Souza, L.E. Fernandez-Outon, J.D. Ardisson, R.M. Lago, Hybrid magnetic amphiphilic composites based on carbon nanotube/nanofibers and layered silicates fragments as efficient adsorbent for ethinyl estradiol, J. Colloid Interface Sci. 379 (2012) 84–88.
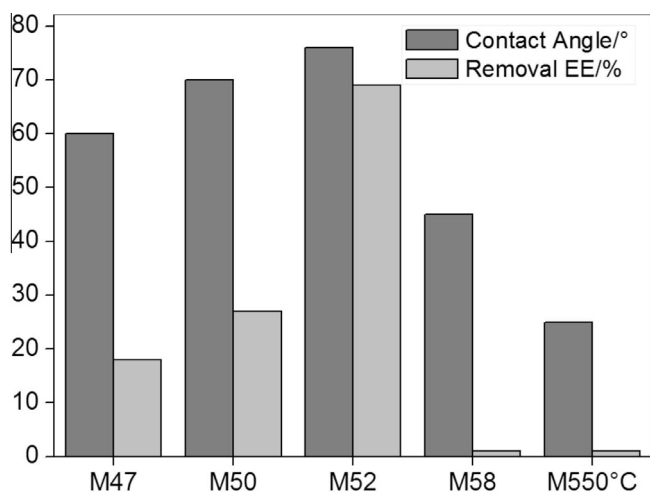
[2] H. Hamid, C. Eskicioglu, Fate of estrogenic hormones in wastewater and sludge treatment: a review of properties and analytical detection techniques in sludge matrix, Water Res. 46 (2012) 5813–5833.

[3] A.N. Fernandes, M. Giovanela, C.A.P. Almeida, V.I. Esteves, M.M.D. Sierra, M.T. Grassi, Removal of the hormones 17 β-estradiol and 17 α-ethinyl estradiol from aqueous solutions employing a decomposed peat as adsorbent material, Quim. Nova 34 (2011) 1526–1533.

[4] B. Pan, D. Lin, H. Mashayekhi, B. Xing, Adsorption and hysteresis of bisphenol A and 17α-ethinyl estradiol on carbon nanomaterials, Environ. Sci. Technol. 42 (2008) 5480–5485.

[5] D.M. Bila, M. Dezotti, Endocrine disrupters in the environment: part 1 – effects and consequences, Quim. Nova 30 (2007) 651–666.

[6] R.W. Reis Filho, J.C.D. Araujo, E.M. Vieira, Sexual estrogenic hormones: bioactive contaminants, Quim. Nova 29 (2006) 817–822.

[7] R. Länge, T.H. Hutchinson, C.P. Croudace, F. Siegmund, H. Schweinfurth, P. Hampe, G.H. Panter, J.P. Sumpter, Effects of the synthetic estrogen 17α-ethinylestradiol on the life-cycle of the fathead minnow (*Pimephales promelas*), Environ. Toxicol. Chem. 20 (2001) 1216–1227.

[8] A. Flores, E.M. Hill, Formation of estrogenic brominated ethinylestradiol in drinking water: implications for aquatic toxicity testing, Chemosphere 73 (2008) 1115–1120.

[9] M.G. Maniero, D.M. Bila, M. Dezotti, Degradation and estrogenic activity removal of 17β-estradiol and 17α-ethinylestradiol by ozonation and O₃/H₂O₂, Sci. Total Environ. 407 (2008) 105–115.

[10] Z. Zhang, J. Hu, Effect of environmental factors on estrogenic compounds adsorption by MIP, Water Air Soil Pollut. 210 (2010) 255–264.

[11] X. Zhang, P. Chen, F. Wu, N. Deng, J. Liu, T. Fang, Degradation of 17α-ethinylestradiol in aqueous solution by ozonation, J. Hazard. Mater. 133 (2006) 291–298.

[12] B. Cunha, W. Botero, L. Oliveira, V. Carlos, M.M. Pompêo, L. Fraceto, A. Rosa, Kinetics and adsorption isotherms of bisphenol A, estrone, 17β-estradiol, and 17α-ethinylestradiol in tropical sediment samples, Water Air Soil Pollut. 223 (2012) 329–336.

[13] D. Carr, A. Morse, J. Zak, T. Anderson, Microbially mediated degradation of common pharmaceuticals and personal care products in soil under aerobic and reduced oxygen conditions, Water Air Soil Pollut. 216 (2011) 633–642.

[14] K.M. Vieira, C.C. Nascentes, R. Augusti, Ozonation of ethinyl estradiol in aqueous-methanolic solution: direct monitoring by electrospray ionization mass spectrometry, J. Braz. Chem. Soc. 21 (2010) 787–794.

[15] S. Canonica, L. Meunier, U. von Gunten, Phototransformation of selected pharmaceuticals during UV treatment of drinking water, Water Res. 42 (2008) 121–128.

[16] L.D. Nghiem, A.I. Schäfer, T.D. Waite, Adsorptive interactions between membranes and trace contaminants, Desalination 147 (2002) 269–274.

[17] W.J. Barr, T. Yi, D. Aga, O. Acevedo, W.F. Harper, Using electronic theory to identify metabolites present in 17α-ethinylestradiol biotransformation pathways, Environ. Sci. Technol. 46 (2011) 760–768.

[18] B. Saha, E. Karounou, M. Streat, Removal of 17β-oestradiol and 17α-ethinyl oestradiol from water by activated carbons and hypercrosslinked polymeric phases, React. Funct. Polym. 70 (2010) 531–544.

[19] D. Zhao, J. Feng, Q. Huo, N. Melosh, G.H. Fredrickson, B.F. Chmelka, G.D. Stucky, Triblock copolymer syntheses of mesoporous silica with periodic 50–300 Angstrom pores, Science 279 (1998) 548–552.

[20] C.T. Kresge, M.E. Leonowicz, W.J. Roth, J.C. Vartuli, J.S. Beck, Ordered mesoporous molecular sieves synthesized by a liquid-crystal template mechanism, Nature 359 (1992) 710–712.

[21] S. Brunauer, P.H. Emmett, E. Teller, Adsorption of gases in multimolecular layers, J. Am. Chem. Soc. 60 (1938) 309–319.

[22] P. Kirkegaard, M. Eldrup, Positronfit extended: a new version of a program for analysing position lifetime spectra, Comput. Phys. Commun. 7 (1974) 401–409.

[23] H. Pan, J.A. Ritter, P.B. Balbuena, Examination of the approximations used in determining the isosteric heat of adsorption from the Clausius–Clapeyron equation, Langmuir 14 (1998) 6323–6327.

[24] D. Barrera, J. Villarroel-Rocha, L. Marenco, M. Oliva, K. Sapag, Non-hydrothermal synthesis of cylindrical mesoporous materials: influence of the surfactant/silica molar ratio, Adsorpt. Sci. Technol. 29 (2011) 975–988.

[25] Y. Feng, Z. Zhang, P. Gao, H. Su, Y. Yu, N. Ren, Adsorption behavior of EE2 (17α-ethinylestradiol) onto the inactivated sewage sludge: kinetics, thermodynamics and influence factors, J. Hazard. Mater. 175 (2010) 970–976.

[26] A.K. Kumar, S.V. Mohan, Endocrine disruptive synthetic estrogen (17α-ethynylestradiol) removal from aqueous phase through batch and column sorption studies: mechanistic and kinetic analysis, Desalination 276 (2011) 66–74.

[27] S. Rovani, M.T. Censi, S.L. Pedrotti Jr., É.C. Lima, R. Cataluña, A.N. Fernandes, Development of a new adsorbent from agro-industrial waste and its potential use in endocrine disruptor compound removal, J. Hazard. Mater. 271 (2014) 311–320.

[28] C. Jung, A. Son, N. Her, K. Zoh, J. Cho, Y. Yoon, Removal of endocrine disrupting compounds, pharmaceuticals, and personal care products in water using carbon nanotubes: a review, J. Ind. Eng. Chem. 27 (2015) 1–11.

[29] C.B. Vidal, M. Seredych, E. Rodríguez-Castellón, R.F. Nascimento, T.J. Bansosz, Effect of nanoporous carbon surface chemistry on the removal of endocrine disruptors from water phase, J. Colloid Interface Sci. 449 (2015) 180–191.

[30] A.P.C. Teixeira, A.D. Purceno, C.C.A. de Paula, J.C.C. da Silva, J.D. Ardisson, R.M. Lago, Efficient and versatile fibrous adsorbent based on magnetic amphiphilic composites of chrysotile/carbon nanostructures for the removal of ethinyl estradiol, J. Hazard. Mater. 248–249 (2013) 295–302.

[31] T. Horikawa, Y. Zeng, D.D. Do, K. Sotowa, J.R.A. Avila, On the isosteric heat of adsorption of non-polar and polar fluids on highly graphitized carbon black, J. Colloid Interface Sci. 439 (2015) 1–6.

[32] I.X. García-Zubiri, G. González-Gaitano, J.R. Isasi, Isosteric heats of sorption of 1-naphthol and phenol from aqueous solutions by β-cyclodextrin polymers, J. Colloid Interface Sci. 307 (2007) 64–70.